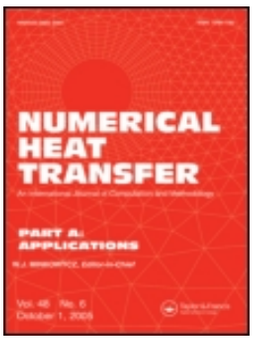

Taylor & Francis
Taylor & Francis Group

Numerical Heat Transfer, Part A: Applications
An International Journal of Computation and Methodology

ISSN: 1040-7782 (Print) 1521-0634 (Online) Journal homepage: http://www.tandfonline.com/loi/unht20

Entropy Generation Due to Natural Convection in a Partially Open Cavity with a Thin Heat Source Subjected to a Nanofluid

Amir Houshang Mahmoudi , Mina Shahi & Farhad Talebi

To cite this article: Amir Houshang Mahmoudi , Mina Shahi & Farhad Talebi (2012) Entropy Generation Due to Natural Convection in a Partially Open Cavity with a Thin Heat Source Subjected to a Nanofluid, Numerical Heat Transfer, Part A: Applications, 61:4, 283-305, DOI: 10.1080/10407782.2012.647990

To link to this article: https://doi.org/10.1080/10407782.2012.647990

Numerical Heat Transfer, Part A, 61: 283–305, 2012

ISSN: 1040-7782 print/1521-0634 online
DOI: 10.1080/10407782.2012.647990

Taylor & Francis
Taylor & Francis Group

ENTROPY GENERATION DUE TO NATURAL CONVECTION IN A PARTIALLY OPEN CAVITY WITH A THIN HEAT SOURCE SUBJECTED TO A NANOFLUID

Amir Houshang Mahmoudi[1,3], Mina Shahi[2], and Farhad Talebi[1]

[1]*Faculty of Engineering, Department of Mechanical Engineering, Semnan University, Semnan, I. R. Iran*
[2]*Laboratory of Thermal Engineering, Faculty of Engineering Technology, University of Twente, Enschede, The Netherlands*
[3]*R&D Department of Oghab Afshan Company, Semnan, I. R. Iran*

This article presents a numerical study of natural convection cooling of a heat source mounted inside the cavity, with special attention being paid to entropy generation. The right vertical wall is partially open and is subjected to copper–water nanofluid at a constant low temperature and pressure, while the other boundaries are assumed to be adiabatic. The governing equations have been solved using the finite volume approach, using SIMPLE algorithm on the collocated arrangement. The study has been carried out for a Rayleigh number in the range $10^3 < Ra < 10^6$, and for solid volume fraction $0 < \varphi < 0.05$. In order to investigate the effect of the heat source and open boundary location, six different configurations are considered. The effects of Rayleigh numbers, heat source and open boundary locations on the streamlines, isotherms, local entropy generation, Nusselt number, and total entropy generation are investigated. The results indicate that when open boundary is located up, the fluid flow augments and hence the heat transfer and Nusselt number increase and total entropy generation decreases.

INTRODUCTION

Heat transfer from open cavities has received considerable attention for its importance in many engineering applications and has been studied extensively in the literature [1–6]. For example, these include cooling of electronic components, open cavity solar thermal receivers, evaporative cooling, and fire control in buildings. Most researchers considered natural convections inside open ended enclosures in contact with pure fluid. However, there is only one study concerning the cooling process in open cavities filled by nanofluid which was done by the authors [7]. In recent years, nanofluids have attracted more attention for cooling in various

Received 3 May 2011; accepted 20 November 2011.
Address correspondence to Amir Houshang Mahmoudi, Faculty of Engineering, Department of Mechanical Engineering, Semnan University, A83 Semnan, I. R. Iran. E-mail: amirhoshangm@gmail.com

NOMENCLATURE

Ec	Eckert number	CW	clockwise
Gr	Grashof number, $\beta g H^4 q''/k\upsilon^2$	CCW	counterclockwise
g	gravitational acceleration, m/s^2	α	thermal diffusivity, $k/(\rho c_p)$, m^2/s
H	height of the cavity, m	β	coefficient of volume expansion, K^{-1}
h_0	height of heat source	ϕ	solid volume fraction
L	width of the cavity, m	μ	dynamic viscosity, $Pa \cdot s$
l_0	width of heat source	υ	kinematics viscosity, m^2/s
k	thermal conductivity, W/mK	ρ	density, kg/m^3
k_b	Boltzmann's constant, 1.38065×10^{-23}	θ	dimensionless temperature
Nu	Nusselt number		
p	pressure, N/m^2		
P	dimensionless pressure,	Subscripts	
Pr	Prandtl number, υ_f/α_f	f	fluid
Ra	Rayleigh number, $\beta g H^4 q''/k\upsilon\alpha$	eff	effective
S_{gen}	entropy generation rate per unit volume, W/m^3 K	m	average
		nf	nanofluid
S^*	dimensionless of entropy generation	p	particle
T	temperature, K	o	reference state
u, v	components of velocity, m/s	s	solid
U, V	dimensionless of velocity component	w	wall
x, y	Cartesian coordinates, m	in	inlet
X, Y	dimensionless of Cartesian coordinates	out	outlet

industrial applications. Such fluids consist of suspended nanoparticles which have a better suspension stability compared to millimeter or micrometer sized ones. Use of metallic nanoparticles with high thermal conductivity will increase the effective thermal conductivity of these types of fluids remarkably. Since nanofluid consists of very small sized solid particles, in low solid concentration it is reasonable to consider nanofluid as a single phase flow [8]. A literature review shows that there are numerous numerical studies on heat transfer by natural convection within cavities filled by nanofluids [9–18]. A numerical study of natural convection of copper–water nanofluid in a two–dimensional enclosure was conducted by Khanafer et al. [9]. The nanofluid in the enclosure was assumed to be in single phase. It was found in any given Grashof number; heat transfer in the enclosure increased with the volumetric fraction of the copper nanoparticles in the water. Sheikhzadeh et al. [10] investigated numerically natural convection within the cavity and considered the effect of position of heat source and heat sink on the sides-wall on the fluid flow and heat transfer. They found the maximum average Nusselt number for high and low Rayleigh numbers occurs for the bottom-middle and the middle-middle locations of the thermally active parts, respectively. Aminossadati et al. [11] studied natural convection cooling of a localized heat source at the bottom of an enclosure. Their results have indicated that adding nanoparticles into pure water improves its cooling performance especially at low Rayleigh numbers. The type of nanoparticles and the length and location of the heat source proved to significantly affect the heat source maximum temperature. Mahmoudi et al. [12] investigated numerically the effect of position of a horizontal heat source on the left vertical wall of a cavity which filled with nanofluid. They found that when the heat source is mounted on the middle of

the left vertical wall, heat transfer and Nusselt number are more than when it is close to the top and bottom horizontal walls.

However, to find the optimal design of thermal systems with minimum loss of available energy, one route is minimization of entropy generation as introduced by Bejan [19]. This method has already been extensively applied to forced and free convection problems, and has been well established in the literature [20–25]. Entropy generation has attracted more attention in many fields such as electronic cooling, turbo machinery, heat exchangers, etc., because it can give good information about loss of energy due to heat transfer and fluid friction irreversibility. Therefore, energy can be saved by reducing this loss.

Entropy generation was mostly analyzed in enclosures filled by conventional fluids (such as water, ethylene glycol, etc.), and the effect of nanoparticles on entropy generation in enclosures has not been adequately investigated. The study of thermal nanofluid flow between parallel disks with special attention to entropy generation has been recently simulated by Feng et al. [26]. Another study was carried out by Li et al. [27] to analyze entropy generation in trapezoidal microchannels for steady laminar flow of pure water and CuO-water nanofluids. They minimized entropy generation in the considered microchannel in terms of most suitable channel aspect ratio and Reynolds number range. Singh et al. [28] analyzed entropy generation due to flow and heat transfer in three different channels: microchannel, minichannel, and a conventional channel with alumina–water nanofluids as the model fluid. Their results showed that whether using the alumina–water with high viscosity as a coolant in microchannels, minichannels, and conventional channels is advisable or not depends on flow regime. They also offered an optimum diameter to minimize the entropy generation rate.

The present article reports a numerical study of entropy generation in thermal nanofluid flow in a square open cavity heated with a protruded heat source, which has potential application in the cooling of electronic equipment. The heat transfer characteristics and the irreversibility generated in the cavity depend on the position of open boundary, aspect ratio of the heater, and the location of the heater. However, in the present study only the effect of heat source locations and position of open boundary on the heat transfer characteristics and irreversibility generation in the cavity are investigated. So, six different cases are considered to find the best situation from a first and second thermodynamic laws point of view. In this article, results are presented in the form of streamlines, isotherms, local entropy generation, average Nusselt number, and total entropy generation.

2. PROBLEM DEFINITION AND MATHEMATICAL FORMULATION

A two-dimensional cavity considered for the present study is shown in Figure 1. The cavity is subjected to an external cold nanofluid entering into the cavity from the right opening boundary. The copper–water nanofluid communicating with the opening is kept at a constant temperature (T_c) and pressure in the entry. The other boundaries are assumed to be adiabatic. Six different configurations which are made as a result of heat source and open boundary location are considered, and the heat transfer, fluid flow, and entropy generation are investigated in each case. The dimension of heat source is kept constant and equal to $l_0/H = 0.1$ and $h_0/H = 0.4$ in whole cases.

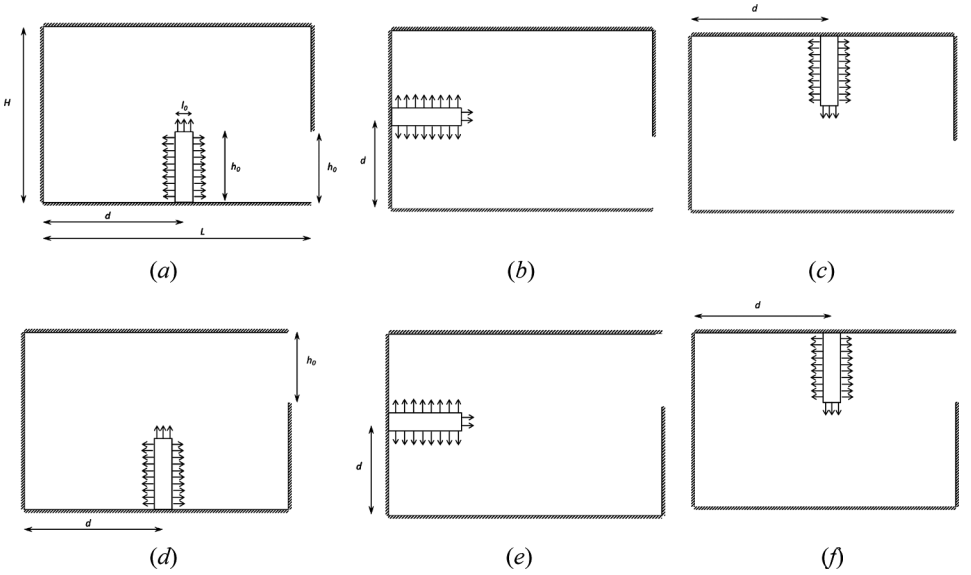

Figure 1. Schematic flow configuration of the studied problems. (*a*) Case 1, (*b*) case 2, (*c*) case 3, (*d*) case 4, (*e*) case 5, and (f) case 6.

It is assumed that both the fluid phase and nanoparticles are in thermal equilibrium and there is no slip between them. Except for the density, the properties of the nanoparticles and fluid are taken to be constant. Table 1 presents thermophysical properties of water and copper at the reference temperature. It is further assumed that the Boussinesq approximation is valid for buoyancy force.

The governing equations (continuity, momentum, and energy equations) and entropy generation for a steady, two-dimensional laminar and incompressible flow are expressed as below:

$$\frac{\partial u}{\partial x}+\frac{\partial v}{\partial y}=0 \tag{1}$$

$$u\frac{\partial u}{\partial x}+v\frac{\partial u}{\partial y}=-\frac{1}{\rho_{nf}}\frac{\partial p}{\partial x}+\upsilon_{nf}\left(\frac{\partial^2 u}{\partial x^2}+\frac{\partial^2 u}{\partial y^2}\right) \tag{2}$$

Table 1. Thermophysical properties of water and copper

Property	Water	Copper
c_p	4,179	383
ρ	997.1	8,954
k	0.6	400
β	2.1×10^{-4}	1.67×10^{-5}

$$u\frac{\partial v}{\partial x}+v\frac{\partial v}{\partial y}=-\frac{1}{\rho_{nf}}\frac{\partial p}{\partial y}+\upsilon_{nf}\left(\frac{\partial^2 v}{\partial x^2}+\frac{\partial^2 v}{\partial y^2}\right)+\frac{g}{\rho_{nf}}(T-T_\infty)[\phi\rho_{s,0}\beta_s+(1-\phi)\rho_{f,0}\beta_f] \tag{3}$$

$$u\frac{\partial T}{\partial x}+v\frac{\partial T}{\partial y}=\alpha_{nf}\left(\frac{\partial^2 T}{\partial x^2}+\frac{\partial^2 T}{\partial y^2}\right) \tag{4}$$

$$S_{gen}=\frac{k_{nf}}{T^2}\left[\left(\frac{\partial T}{\partial x}\right)^2+\left(\frac{\partial T}{\partial y}\right)^2\right]+\frac{\mu_{nf}}{T}\left[2\left\{\left(\frac{\partial u}{\partial x}\right)^2+\left(\frac{\partial v}{\partial y}\right)^2\right\}+\left(\frac{\partial u}{\partial y}+\frac{\partial v}{\partial x}\right)^2\right] \tag{5}$$

where $\alpha_{nf}=k_{nf}/(\rho c_p)_{nf}$.

2.1. Nanofluid Properties

The effective density of nanofluid at the reference temperature can be defined as follows.

$$\rho_{nf,0}=(1-\phi)\rho_{f,0}+\phi\rho_{s,o} \tag{6}$$

where $\rho_{nf,0}$, $\rho_{f,0}$, $\rho_{s,0}$, and ϕ are the density of nanofluid, density of base fluid, density of nanoparticle and volume fraction of the nanoparticles, respectively.

The heat capacitance of nanofluid can be given as follows.

$$(\rho c_p)_{nf}=(1-\phi)(\rho c_p)_f+\phi(\rho c_p)_s \tag{7}$$

The effective thermal conductivity of nanofluid was given by Patel et al. [29] as follows.

$$\frac{k_{eff}}{k_f}=1+\frac{k_p A_p}{k_f A_f}+ck_p\mathrm{Pe}\frac{A_p}{k_f A_f} \tag{8}$$

where c is constant and must be determined experimentally (for the current study $c=3.6\times10^4$), A_p/A_f and Pe are defined as

$$\frac{A_p}{A_f}=\frac{d_p}{d_f}\frac{\phi}{(1-\phi)}\quad \mathrm{Pe}=\frac{u_p d_p}{\alpha_f} \tag{9}$$

where d_p is diameter of solid particles and in this study is assumed to be equal to 100 nm, d_f is the molecular size of liquid that is taken as 2 Å for water. Also, u_p is the Brownian motion velocity of nanoparticle which is defined as

$$u_p=\frac{2k_b T}{\pi\mu_f d_p^2} \tag{10}$$

where k_b is the Boltzmann constant.

The effective viscosity of nanofluid was introduced by Brinkman [30], as below.

$$\mu_{nf} = \frac{\mu_f}{(1-\phi)^{2.5}} \tag{11}$$

2.2. Boundary Conditions

The boundary conditions are in the following forms.

$$\text{At cavity walls: } u = v = 0 \tag{12}$$

$$\text{At cavity walls: } \frac{\partial T}{\partial n} = 0 \tag{13}$$

$$\text{At the heat source's surface: } \begin{cases} u = v = 0 \\ \frac{\partial T}{\partial n} = -q''/k \end{cases}$$

At the open boundary:

$$\begin{cases} T_{in} = T_C,\ \left.\frac{\partial T}{\partial x}\right|_{out} = 0 & \text{at } x = L\ \ 0 \le y \le 0.4H\ \ (cases\ 1, 2, and\ 3) \\ & 0.6H \le y \le H\ \ (cases\ 4, 5, and\ 6) \\ \frac{\partial v}{\partial x} = 0,\ \frac{\partial u}{\partial x} = -\frac{\partial v}{\partial y} & \text{at } x = L\ \ 0 \le y \le 0.4H\ \ (cases\ 1, 2, and\ 3) \\ & 0.6H \le y \le H\ \ (cases\ 4, 5, and\ 6) \end{cases}$$

In order to estimate the heat transfer enhancement, we have calculated Nu (Nusselt number) and Nu_m (average Nusselt number) for the heat source wall as follows.

$$Nu = \left.\frac{1}{\theta}\right|_{\text{fin surfaces}} \tag{14}$$

$$NU_m = \frac{\int_{\text{fin surfaces}} \text{Nu}\ dn}{\int_{\text{fin surfaces}} dn} \tag{15}$$

Equations (1)–(4) can be converted to dimensionless forms by definition of the following parameters.

$$X = \frac{x}{H},\quad Y = \frac{y}{H},\quad U = \frac{uH}{\alpha_f},\quad V = \frac{vH}{\alpha_f},\quad \theta = \frac{(T - T_C)k_f}{q''H},\quad P = \frac{p}{\rho_{nf}}\frac{H^2}{\alpha_f^2} \tag{16}$$

Therefore, using the above parameters leads to dimensionless forms of the above equations as below:

$$\frac{\partial U}{\partial X} + \frac{\partial V}{\partial Y} = 0 \tag{17}$$

$$U\frac{\partial U}{\partial X}+V\frac{\partial U}{\partial Y}=-\frac{\partial P}{\partial X}+\frac{\mu_{nf}}{\rho_{nf}\alpha_f}\left(\frac{\partial^2 U}{\partial X^2}+\frac{\partial^2 U}{\partial Y^2}\right) \tag{18}$$

$$U\frac{\partial V}{\partial X}+V\frac{\partial V}{\partial Y}=-\frac{\partial P}{\partial Y}+\frac{\mu_{nf}}{\rho_{nf}\alpha_f}\left(\frac{\partial^2 V}{\partial X^2}+\frac{\partial^2 V}{\partial Y^2}\right)+Ra\cdot\Pr\cdot\frac{\rho_{f,0}}{\rho_{nf,0}}\left(1-\phi+\phi\frac{\rho_s\beta_s}{\rho_f\beta_f}\right)\theta \tag{19}$$

$$U\frac{\partial \theta}{\partial X}+V\frac{\partial \theta}{\partial Y}=\frac{\alpha_{nf}}{\alpha_f}\left(\frac{\partial^2 \theta}{\partial X^2}+\frac{\partial^2 \theta}{\partial Y^2}\right) \tag{20}$$

The dimensionless form of local entropy generation can be expressed as follows.

$$S^*_{gen}=\frac{k_{nf}}{k_f}\cdot\frac{1}{(\theta+T^*)^2}\left[\left(\frac{\partial\theta}{\partial X}\right)^2+\left(\frac{\partial\theta}{\partial Y}\right)^2\right]+\frac{1}{\theta+T^*}\cdot\frac{\mu_{nf}}{\mu_f}\cdot Ec\cdot\Pr\cdot\left[2\left\{\left(\frac{\partial U}{\partial X}\right)^2+\left(\frac{\partial V}{\partial Y}\right)^2\right\}+\left(\frac{\partial U}{\partial Y}+\frac{\partial V}{\partial X}\right)^2\right] \tag{21}$$

where T^*, S^*_{gen} and Ec are defined as follows.

$$T^*=\frac{Tc.k_f}{q''\cdot H}\quad S^*_{gen}=S_{gen}\cdot\frac{H^2}{k_f}\quad \mathrm{Ec}=\frac{\alpha_f^2\cdot k_f}{H^3\cdot Cp_f\cdot q''}$$

3. NUMERICAL METHOD

The dimensionless equations have been solved numerically based on the finite volume method using a collocated grid system. A central difference scheme is used to discretize the diffusion terms, whereas upwind is adopted for the convection terms. The resulting discretized equations have been solved iteratively through the strongly implicit procedure (SIP) [31]. The SIMPLE algorithm [32] has been adopted for the pressure velocity coupling. More details of the discretization and computational procedure can be found in the literature [33]. To check the convergence of the sequential iterative solution, the sum of the absolute differences of the solution variables between two successive iterations has been calculated When this summation falls below the convergence criterion, convergence is obtained (the convergence criterion has been chosen as 10^{-6} in this study). To allow a grid-independent examination, the numerical procedure has been conducted for different grid resolutions. Table 2 demonstrates the influence of the number of grid points for a test case of fluid confined within the present configuration. From this table it is clear that the grid system of 113×71 is good enough to obtain accurate results.

First, the governing equations have been solved for the natural convection flow in an enclosed cavity filled by pure fluid in order to compare the results with those,

Table 2. Result of grid independence examination

Number of grids in $X-Y$	Nu
73×31	2.39
83×41	2.297
93×51	2.256
103×61	2.226
113×71	2.209
123×81	2.205

Table 3. Comparison of results obtained in this study by reference [34]

	Nu		
	Present	de Vahl Davis [34]	Error (%)
$Ra = 10^4$	2.248	2.242	0.267
$Ra = 10^5$	4.503	4.523	0.444
$Ra = 10^6$	9.147	9.035	1.24

Table 4. Percentage increase in average Nusselt number with respect to clear fluid for different Reynolds number

	Percentage increase in average Nusselt number with respect to clear fluid		
	Present study	Santra et al. [35]	Error
$Re = 100$	18.31	19.02	0.039
$Re = 500$	29.86	31.13	0.042
$Re = 1000$	30.59	31.75	0.037
$Re = 1500$	30.92	32.12	0.038

obtained by de Vahl Davis [34]. This comparison revealed good agreement between the results, which are shown in Table 3. Another test for validation of this code has been performed for the case of isothermally heated parallel plates filled by copper–water nanofluid. In this test case, the results have been compared with those of Santra et al. [35], as shown in Table 4. Also, good agreement with the results was found by the authors [7].

4. DISCUSSION AND RESULTS

In this article, the natural convection flow inside the square cavity heated with a protruded heat source is numerically investigated. To consider the effect of the heat source placement and open boundary position, a study has been carried out for six different cases; in each case the location of the heat source was changed. The numerical computation was performed for a range of Ra and φ ($Ra = 10^3 - 10^6$, $0 < \varphi < 0.05$). In the following, entropy generation due to heat transfer and fluid

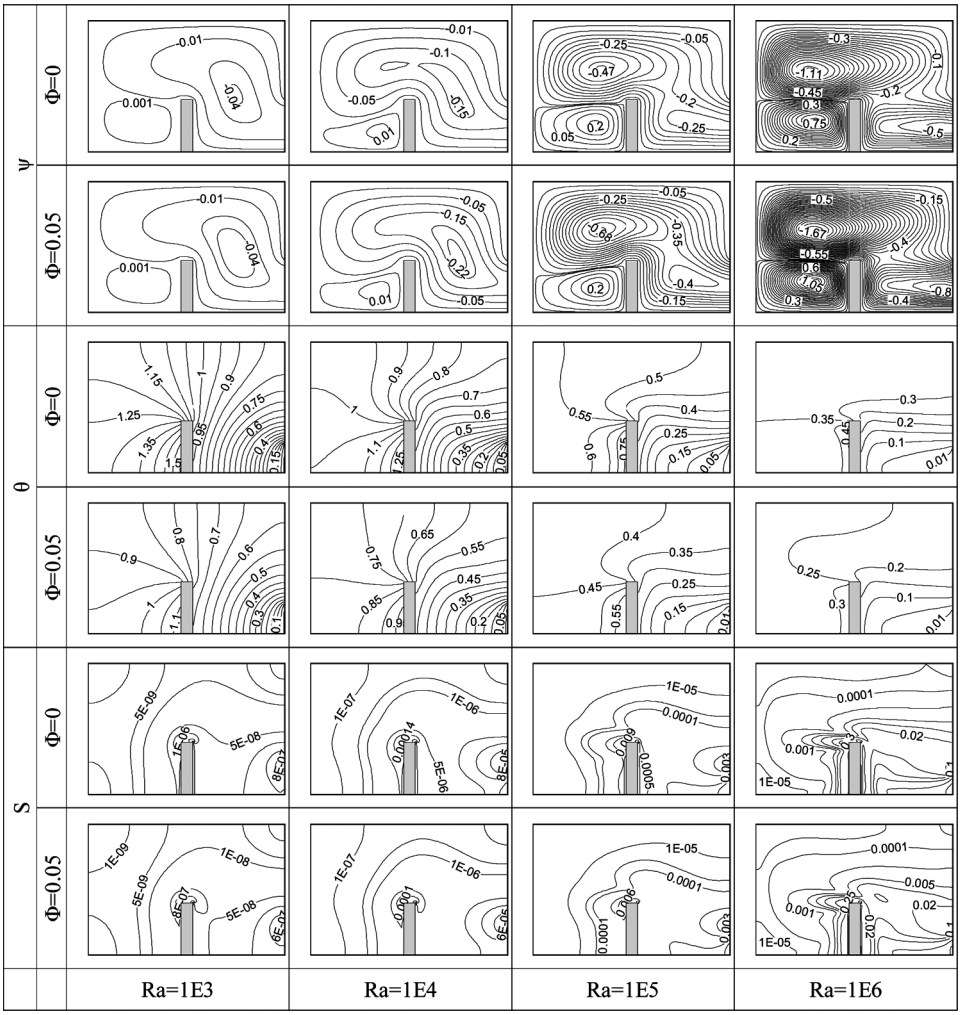

Figure 2. Streamlines, isotherms, and local entropy generation at case 1 for different Rayleigh numbers, $\varphi = 0$, 0.05, and $d = 0.75$.

friction irreversibilities as a function of Ra and solid concentration and heat source location is studied.

In Figure 2, results are presented at different Rayleigh numbers, and $d = 0.75$ for both pure fluid and nanofluid with $\varphi = 5\%$. As can be seen, the cold flow enters the cavity from the bottom portion of the open boundary and after contact with the heat source and absorbing heat, moves up and finally exists from the top portion of the open boundary. A clockwise (CW) open recirculation cell forms which covers most of the cavity. At the left side of the heat source, a small counter clockwise (CCW) vortex forms, which is weaker with respect to the major flow in the cavity. At $\mathrm{Ra} = 10^3$ the flow is so much weaker then it is conduction dominant, the parallel isotherms point to this behavior. By increasing the Rayleigh number, flow intensity

augments so heat transfer as a result of enhancement convection heat transfer increases and, hence, temperature in the cavity decreases. At $Ra = 10^6$ the entrance flow which has a significant intensity after contact with the heat source is divided into two parts. The first part turns to the open boundary and leaves the cavity, and the second part after passing from the heater surface and having contact with the CCW vortex, goes around the cavity and finally leaves it from the top portion of the open boundary. So, the whole cavity is covered by three recirculation cells. The presence of nanoparticles in the water enhances the effective thermal conductivity and leads to the increase in intensity of flow as a result of the augmentation in the buoyancy force. Nanoparticles have a stronger effect on flow intensity at $Ra = 10^6$, so that with 5% solid concentration the value of stream function increases about 50%.

Entropy generation in the cavity is due to two factors: heat transfer and fluid friction irreversibilities. As can be seen in Figure 2, in all Rayleigh values the local entropy generation rate is higher near the heater due to the existence of severe temperature gradient; but far apart from the heater, it becomes less. It is also clear that with increasing Rayleigh number, the local entropy generation due to the existence of larger temperature gradients and enhanced velocity levels, and so the stronger fluid friction in these mentioned areas, becomes significant. Adding the copper nanoparticles to the base fluid has two opposed effects: 1) increasing the viscosity of fluid it leads to an increase in viscous dissipation, so it results in an increasing of entropy generation; and 2) augmenting the thermal conductivity, it can enhance the heat transfer rate and causes a reduction in the entropy generation as a result of the existence of smaller temperature gradient. These two opposing effects of the presence of nanoparticles lead to a decrease in local entropy generation within the enclosure, and the value of local entropy at the top-left corner of heat source in $Ra = 10^6$ with 5% solid concentration decreases from 0.3 to 0.25. Correspondingly, using nanofluids leads to better performance efficiencies when compared to pure water.

Figure 3 shows streamlines, isotherms, and local entropy generation for different heat source positions along the bottom horizontal wall (case 1) at $Ra = 10^5$ and $\varphi = 0, 0.05$. At $d = 0.35$, the entrance flow after passing parallel with bottom horizontal wall, covers the left vertical heat source wall, goes up, and finally leaves the cavity from the top portion of the open boundary. A CW open recirculation cell then forms which covers most of the cavity. Also, a small CCW vortex forms between the heat source and left vertical wall of the cavity. As can be seen in Figure 3 the flow configuration changes with location of the heat source. By coming nearer to the heat source to the open boundary, a portion of entrance flow after contact with the heat source turns back to the open boundary and leaves the cavity, so less cold flow comes within the cavity. So that at $d = 1.25$ most of the entrance flow leaves the cavity immediately after contact with the heater, and it leads to separate vortex forms on the top of the heat source. By moving the heat source toward the open boundary due to enhancement of resistance against entrance flow, the inlet mass flow rate lessens and hence the heat transfer decreases so that at $d = 1.25$, although the heater is closer to the heat sink temperature is higher than other values of d in this case. At $d = 0.65$, due to the distance of the heat source with the left vertical wall of the cavity being more than $d = 0.35$, the CCW recirculation cell becomes larger and heat

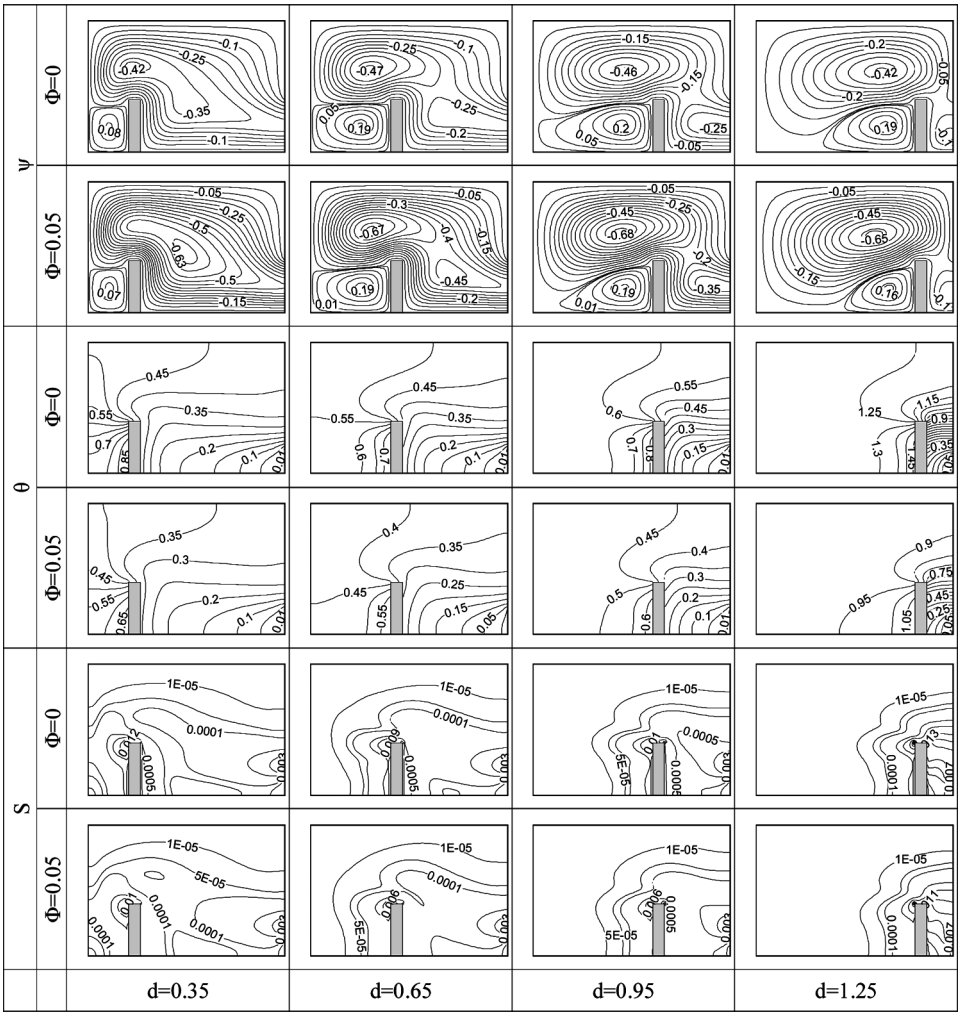

Figure 3. Streamlines, isotherms, and local entropy generation for different heat source positions along the south horizontal wall (case 1) at $Ra = 10^5$ and $= 0, 0.05$.

transfer from the left surface of the heater increases and so the temperature decreases. At $d = 0.95$, although the vortex at the left side of the heater is stronger and has a longer boundary with a major recirculation cell, the inlet mass flow rate decreases and causes a reduction in heat transfer so the temperature increases in comparison with $d = 0.65$. In this case, the presence of nanoparticles has the most effect on the flow intensity at $d = 1.25$, so that by 5% solid concentration the value of stream function grows to about 55%.

At $d = 0.35$, due to the existence of weak heat transfer at the top-left corner of the heat source, there is a strong temperature gradient there so the value of local entropy is high. By moving the heat source to the right side, at first the local entropy at the left side of heater decreases ($d = 0.65$) but at higher value of d the local entropy

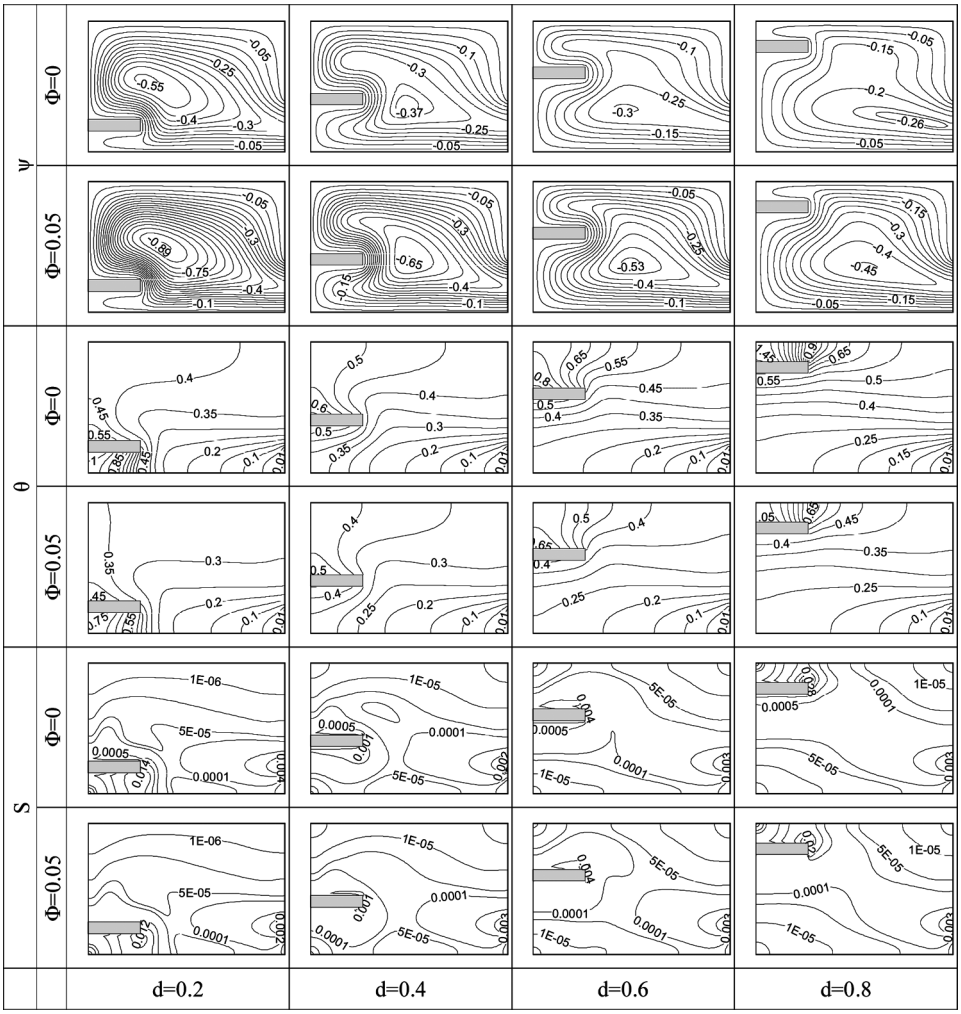

Figure 4. Streamlines, isotherms, and local entropy generation for different heat source positions along the left vertical wall (case 2) at $\mathrm{Ra} = 10^5$ and $\varphi = 0$, 0.05.

grows again so that at$d = 1.25$, the local entropy at the top-right corner of the heat source is about 0.013.

In Figure 4, results are presented for different heat source positions along the left vertical wall (case 2) at $\mathrm{Ra} = 10^5$ for both pure fluid and nanofluid with $\varphi = 0.05$. At $d = 0.2$, the cold flow enters the cavity parallel to the bottom horizontal wall and penetrates a little in the gap between the heat source and bottom wall of the cavity, then it turns up, and finally goes out from the open boundary. So an open CW recirculation cell forms which covers the whole cavity. By moving the heat source up, the flow intensity decreases and the position of the center of the recirculation cell change from the top to bottom of the heat source. By changing the position of the heat source from $d = 0.2$ to $d = 0.6$ due to an increase in the flow

intensity near the bottom surface of the heater, the convection increases and hence temperature decreases, but at $d = 0.8$ the temperature at the bottom of the heater grows. This is due to the fact that at $d = 0.8$, the flow intensity in the whole cavity is very weak and it causes heat transfer from all surfaces of the heater to decrease, so that at $d = 0.8$ the maximum temperature in this case occurs on the top of the heat source. In this case, existence of nanoparticles is more effective on flow intensity at $d = 0.4$ and 0.6, so that by 5% solid concentration the value of stream function increases about 76%.

With a short distance between the heat source and the bottom horizontal wall of the cavity and the temperature gradient is high, so the local entropy is also high at the bottom of the heat source. By moving the heat source up, the value of the local

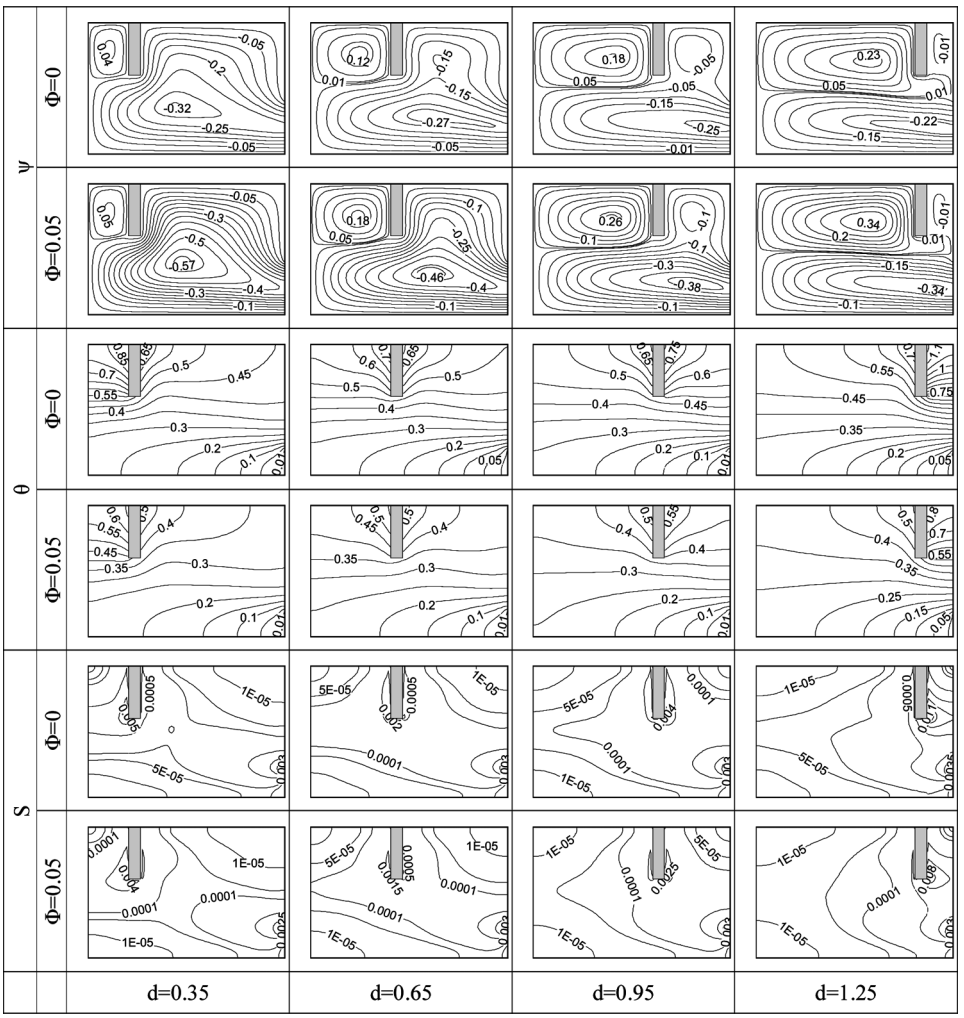

Figure 5. Streamlines, isotherms, and local entropy generation for different heat source positions in case 3 at $\mathrm{Ra} = 10^5$ and $\varphi = 0$, 0.05.

entropy decreases at the bottom of the heater and increases on the top of it. In this case, the highest value of local entropy happens at $d = 0.8$.

Figure 5 shows streamlines, isotherms, and local entropy generation for different heat source positions along the top horizontal wall (case 3) at $\mathrm{Ra} = 10^5$and $\varphi = 0, 0.05$. At $d = 0.35$, the inlet flow after passing the whole cavity except the gap between the heat source and the left vertical wall of the cavity which is occupied by a small CCW vortex, leaves the cavity from the top portion of the open boundary and forms an open CW recirculation cell. By moving the heater to the right side, flow intensity in the CW recirculation cell becomes weaker and hence heat transfer from the right wall of the heat source which is in contact with this recirculation flow decreases and temperature increases. On the other side, by increasing the CCW vortex at the left side of the heater becomes stronger and leads to an enhancement in heat transfer from the left heater wall. By moving the heat source to the right side a small change happens in flow configuration and a new center appears at the right side of the heat source. At $d = 1.25$, it changes to a separate CW vortex within the gap between the heat source and the right vertical wall. Due to the absence of a direct contact between the cold inlet flow and the right wall of the heater, heat transfer from this surface decreases deeply and temperature increases. The presence of nanoparticles has more of an effect on flow intensity in this case in comparison with case 1. The maximum effect occurs at $d = 0.35$ with a 78% increase in stream function as a result of 5% solid concentration.

Figure 6 shows streamlines, isotherms, and local entropy generation for different heat source positions along the bottom horizontal wall when the open boundary is located on the top of the right vertical cavity wall (case 4) at $\mathrm{Ra} = 10^5$ and $\varphi = 0, 0.05$. In this case, the cavity surface is covered with a small CCW vortex at the left side of the heat source and a large open CW recirculation cell. By increasing, flow intensity of the CW recirculation cell decreases but the CCW vortex augments. In this case, flow is stronger than in case 1 in all values of d, so that at $d = 0.35$ the stream function value in the middle of the CW recirculation cell in case 4 is 86% higher than case 1. Contrary to case 1, by moving the heat source toward the open boundary the inlet mass flow rate didn't change significantly. With the augmentation of the CCW vortex as a result of going to the heater far from the left vertical wall, the temperature at the left side of the heater decreases. At $d = 1.25$, temperature at the left heater wall is 0.45 which is the lowest value between other values of d but at case 1 temperature in this area is about 1.45 which is the highest value with respect to other values of d in that case. In comparison with case 1, the temperature gradient around the heat source is lower as a result of stronger flow and convection heat transfer, so local entropy generation decreases. For instance at $d = 1.25$, the local value of entropy generation at the top-left corner of the heat source at case 1 is about 0.013 but it decreases to 0.009 at case 4.

Streamlines, isotherms, and local entropy generation at $\mathrm{Ra} = 10^5$ and $\varphi = 0, 0.05$ are illustrated in Figure 7 for the fifth configuration (case 5). In comparing to Figure 4 it is clear that flow is stronger when the open boundary is located at the top portion of the left vertical wall, so that at $d = 0.2$ the value of stream function at case 5 is higher at about 56% with respect to case 2. This is due to the fact that when the open boundary is located at the top of the left vertical wall, the hot upward flow in order to exit from the cavity shouldn't turn downward, similar to case 2, so it

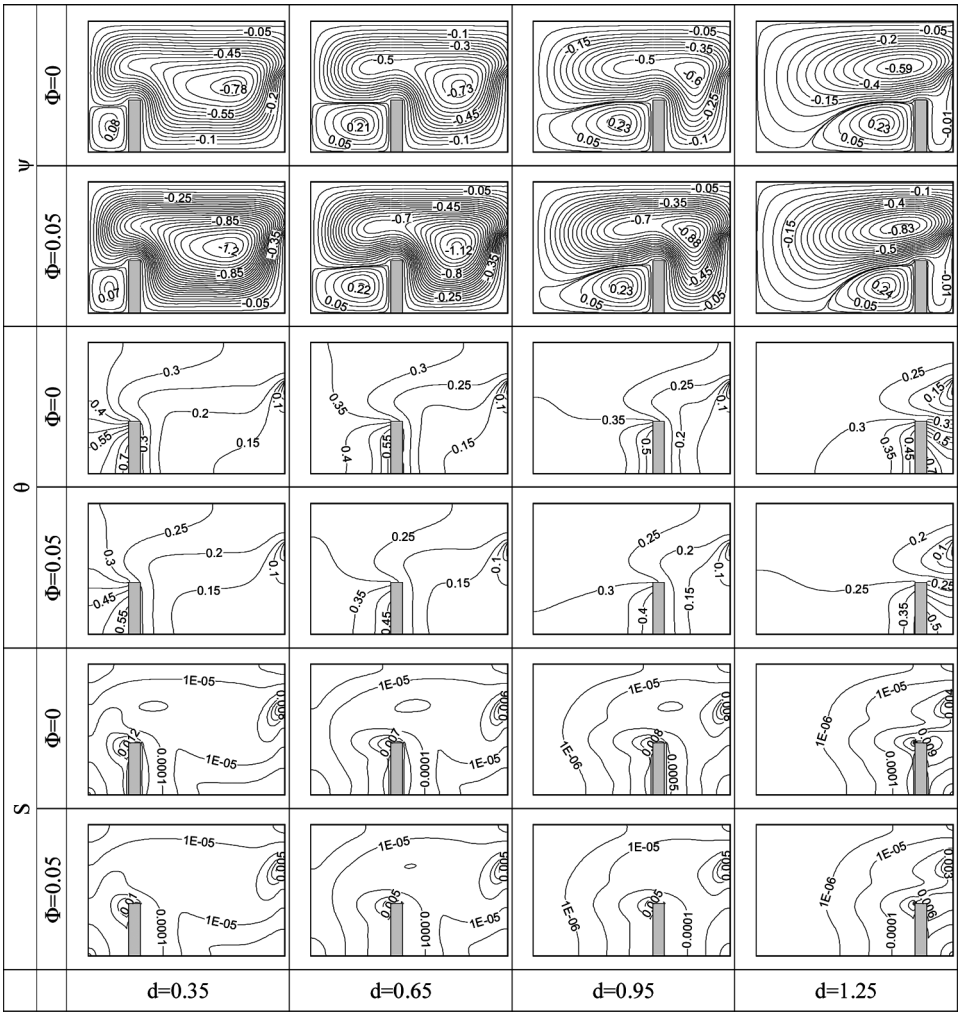

Figure 6. Streamlines, isotherms, and local entropy generation for different heat source positions along the south horizontal wall when the open boundary is up (case 4) at $\mathrm{Ra} = 10^5$ and $= 0$, 0.05.

leads to a decrease in resistance against the flow and hence recirculation flow augments. Higher flow intensity causes better heat transfer then in all values of d, and in case 5 the temperature is lower than case 2. In this case, like case 2, by moving the heat source up the flow becomes weaker but the position of the recirculation cell center doesn't change significantly, contrary to case 2. The presence of nanoparticles has a significant effect on flow intensity but with respect to case 2 its effect is lower. For instance, at $d = 0.4$ with 5% solid concentration the value of stream function in case 2 increases about 76%, but in case 5 it increases a mere 54%.

Figure 8 shows streamlines, isotherms, and local entropy generation for different heat source positions along the top horizontal wall (case 6) at $\mathrm{Ra} = 10^5$ and $\varphi = 0, 0.05$. By moving the heat source to the right side, the CW recirculation flow

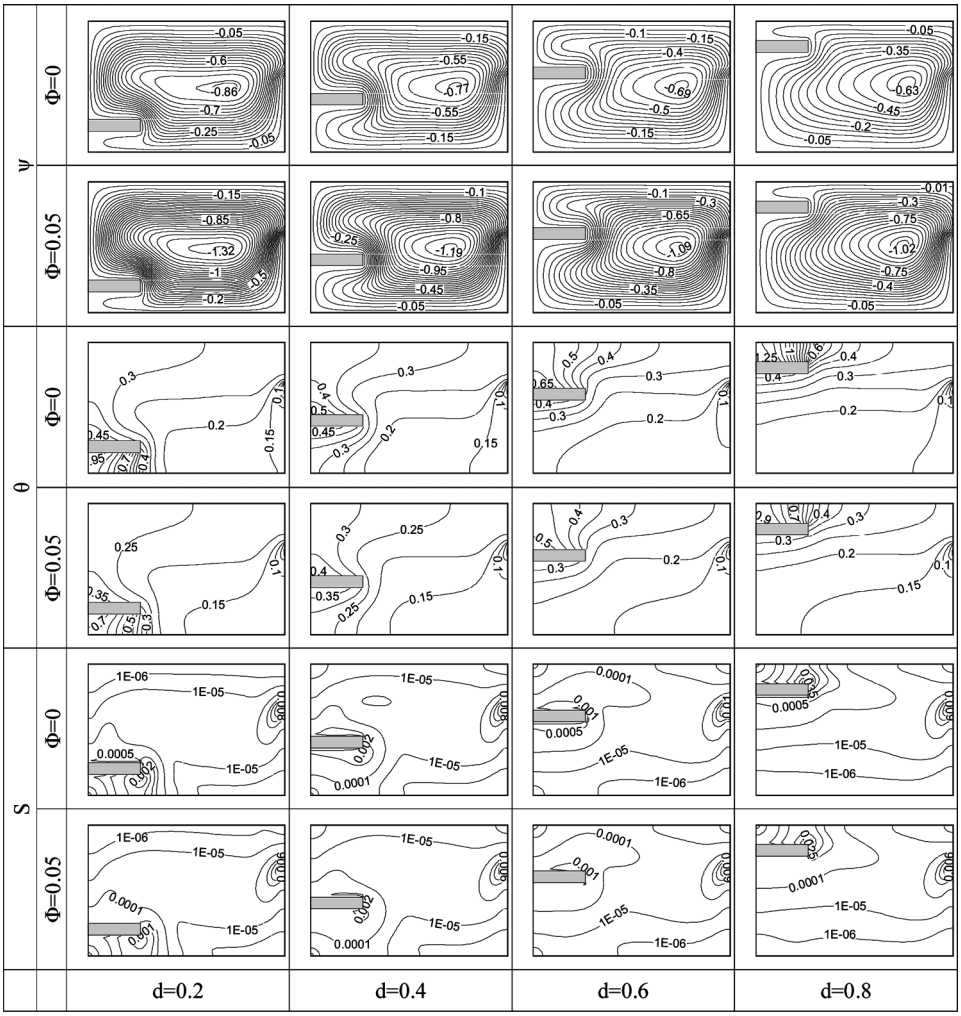

Figure 7. Streamlines, isotherms, and local entropy generation for different heat source positions in case 5 at $\mathrm{Ra} = 10^5$ and $=0$, 0.05.

becomes weaker but the CCW vortex at the left side of the heater becomes stronger so heat transfer from the left heater wall increases and leads to the reduction of temperature in that area. By getting nearer to the heat source to the open boundary due to enhancement of resistance against the inlet and outlet flows, the inlet mass flow rate decreases and leads to a decreased convection heat transfer, so that at $d = 1.25$ although the heat source is very close to the heat sink but because of the decrease in heat transfer as a result of reduction in inlet mass flow rate, temperature increases with respect to the $d = 0.95$. In comparison with case 3, it is clear that flow intensity is higher at case 6, so it leads to enhancement of heat transfer and reduction in temperature gradient and local entropy generation. Like case 5, the presence of

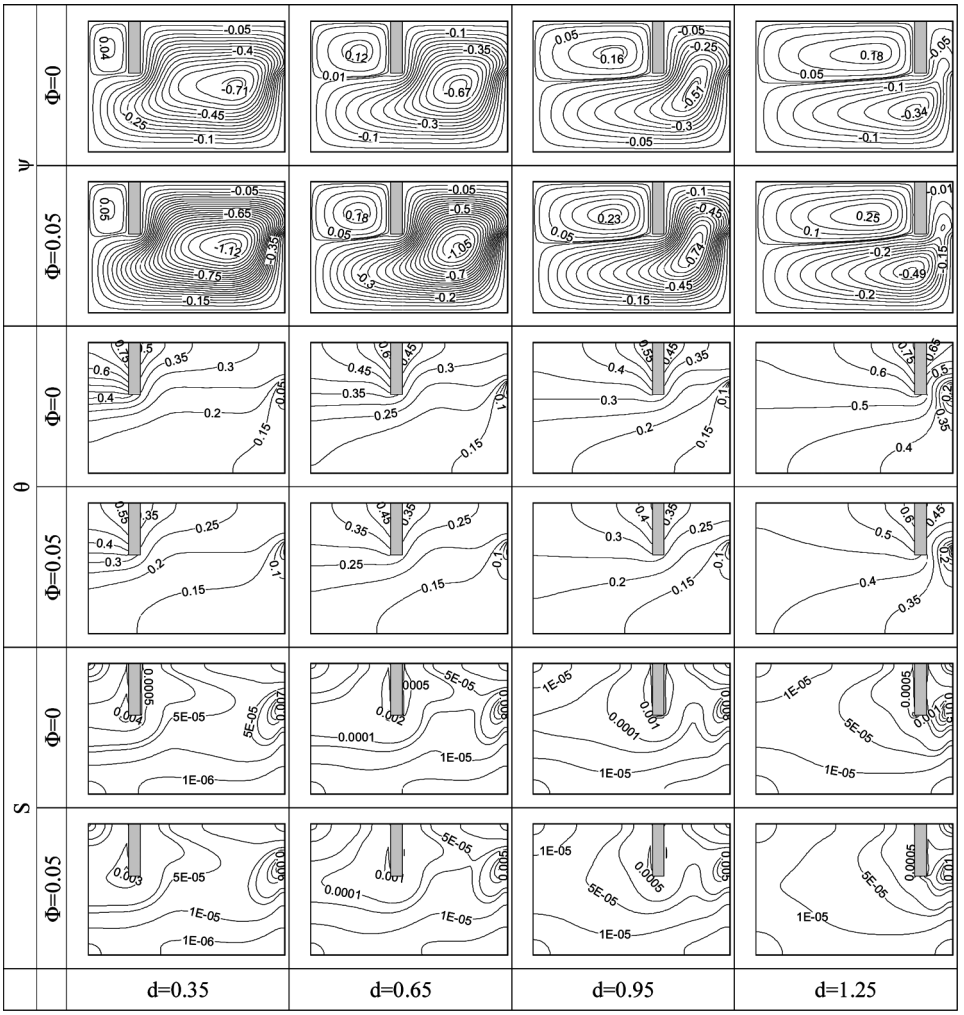

Figure 8. Streamlines, isotherms, and local entropy generation for different heat source positions in case 6 at $\mathrm{Ra} = 10^5$ and $\varphi = 0$, 0.05.

metallic nanoparticles when the open boundary comes up has a lower effect on the flow intensity.

Figure 9 displays the effect of solid concentration on the variation of the average Nusselt number on the heat source surface and the total entropy generation for different values of Rayleigh number in case 1 and $d = 0.75$. As can be expected with the increasing of the Rayleigh number, convective heat transfer and hence the Nusselt number increase. Existence of the metallic nanoparticles when increasing the thermal conductivity of the mixture causes an enhancement in heat transfer, when can be seen in Figure 9*a*, the value of the average Nusselt number increases. Nanofluid has more effect on Nu at a lower Rayleigh number due to the conduction scheme is more important in heat transfer from heat source to cold inlet flow. So, that at $\mathrm{Ra} = 10^3$ with 5%

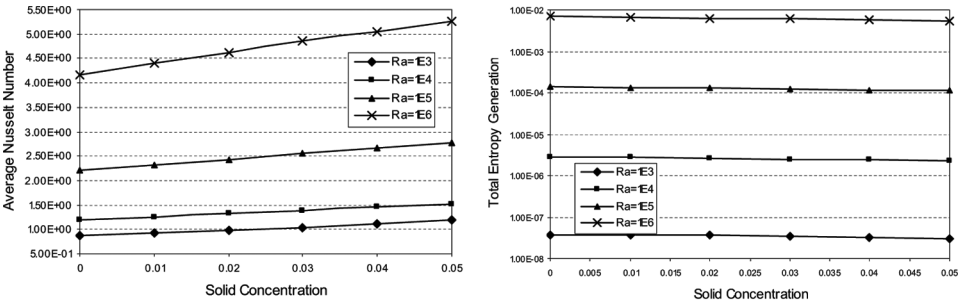

(*a*) (*b*)

Figure 9. Effect of solid concentration on the variation of (*a*) the average Nusselt number, and (*b*) the total entropy generation for different values of Rayleigh numbers in case 1.

solid concentrations the average Nusselt number increases about 36%, but at $\mathrm{Ra} = 10^6$ it increases 26%. With increasing the Rayleigh number, more energy enters the cavity so the temperature gradient grows. In addition, flow velocity and friction loss increases, so the total entropy generation increases. The presence of nanoparticles makes the temperature distribution more uniform and it leads to a reduction in entropy generation. For instance at $\mathrm{Ra} = 10^3$, 5% increase of solid concentration reduces the total entropy generation approximately 20%.

Figure 10 displays the variation of the average Nusselt number on the heat source surface against the solid concentration at different spacing for each case when $\mathrm{Ra} = 10^5$. In all cases, when the heat source is close to the cavity walls due to weak flow between the heat source and wall, heat transfer and the average Nusselt number decrease, especially in cases 1, 3, 4, and 6 the lowest Nu occurs at $d = 1.25$. As can be seen in Figure 10*a* although the average Nusselt number increases by moving the heater from $d = 0.65$ to $d = 0.95$, this is smaller than when it moves from $d = 0.35$ to $d = 0.65$. This is due to the fact that despite augmentation of the vortex at the left side of the heat source and becoming nearer to the heat sink by an increase of d, the inlet mass flow rate as it is described in Figure 3 decreases and hence the amount of Nusselt enhancement decreases. When the heat source is attached to the top and horizontal walls of the cavity except case 3, the highest Nu happens at $d = 0.95$. In case 3, although by moving the heater from $d = 0.65$ to $d = 0.95$ the vortex at the left side of the heater augments but due to forming a separate vortex close to the right heater wall, direct contact of cold inlet flow with the heat source is reduced and hence heat transfer and the average Nusselt number decreases. The effect of the presence of nanoparticles on the enhancement of Nusselt is higher in case 3 with respect to cases 1 and 2. This happens for case 5 against cases 4 and 6.

Generally, when the open boundary is located at the top of the left vertical wall due to an increase of flow intensity, heat transfer and hence average Nusselt number grows but the effect of nanoparticles is reduced. For instance at case 2 and $d = 0.8$, 5% solid concentration enhances the average Nusselt number about 35%, but at case 5 it increases about 28%. As a conclusion it is noticeable to say, Nu is in both positions of the open boundary when the heat source mounted on the left vertical wall is higher than when it is on the top or bottom of the horizontal wall.

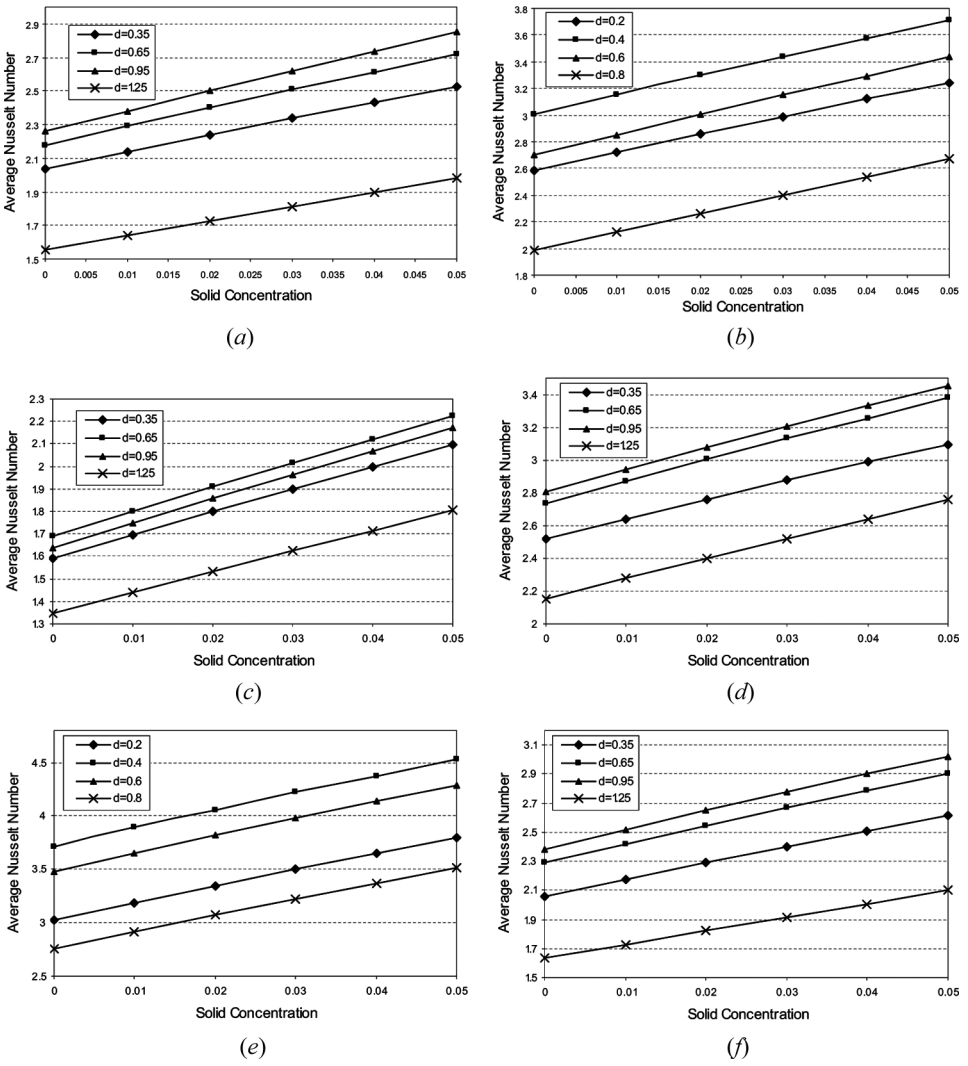

Figure 10. Variation of the average Nusselt number against the solid concentration at different dimensionless spacing at $\mathrm{Ra} = 10^5$ for (*a*) case 1, (*b*) case 2, (*c*) case 3, (*d*) case 4, (*e*) case 5, and (*f*) case 6.

Figure 11 presents the variation of the total entropy generation in the cavity against the solid concentration at different spacing for each case when $\mathrm{Ra} = 10^5$. As described above, whichever heater goes nearer to the cavity walls, heat transfer decreases and hence temperature gradient increases and so entropy generation grows. When the open port is located at the top portion of the left vertical wall, as shown in Figure 10, heat transfer increases and it reduces the total entropy generation. For instance at $d = 1.25$, the total entropy generation in case 4 is approximately 42% lower than case 1. The lowest value of total entropy when the open boundary is at the bottom and top, respectively, happens at cases 1 and 4 which with

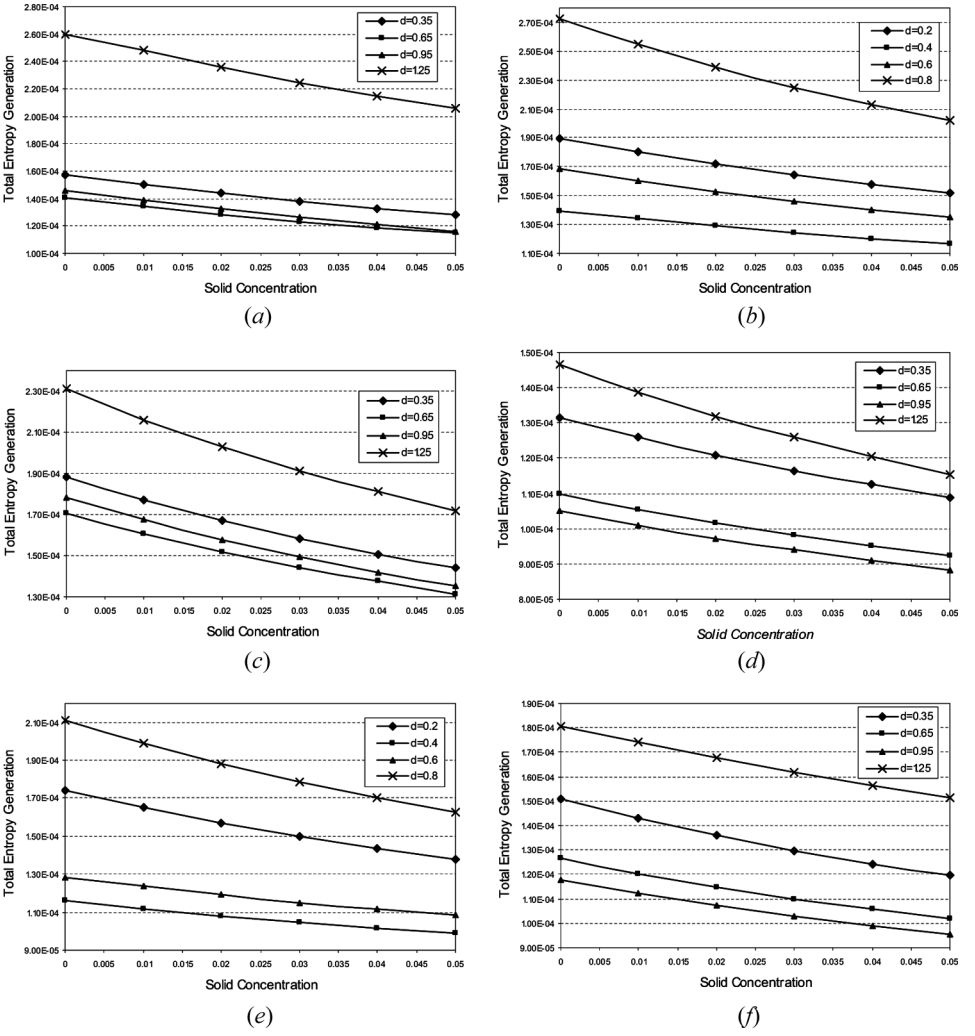

Figure 11. Variation of total entropy generation against the solid concentration at different dimensionless spacing at $Ra = 10^5$ for (*a*) case 1, (*b*) case 2, (*c*) case 3, (*d*) case 4, (*e*) case 5, and (*f*) case 6.

the heat source mounted on the bottom horizontal wall means from the second thermodynamic law these cases are optimum. The presence of nanoparticles has the most effect on the reduction of entropy at case 3, so that with 5% solid concentration total entropy at $d = 1.25$ decreases about 26%.

5. CONCLUSION

The numerical code developed here is used to calculate the entropy generation due to the natural convection cooling of a heat source mounted inside a square partially open cavity filled by copper-water nanofluid for $10^3 < Ra < 10^6$ and volume

fraction of nanoparticles ($0<\varphi<0.05$). Study has been carried out for six cases, and in each case the heater was located in different locations and spacing: Obtained results released some important points, as follows.

- By moving the open boundary to the top portion of left vertical wall, the average Nusselt number and total entropy generation increase but the effect of nanoparticles decreases.
- The maximum value of the average Nusselt number at $\mathrm{Ra} = 10^5$ is obtained for case 5 when the heater is located at a dimensionless spacing of 0.4.
- The minimum value of the average Nusselt number at $\mathrm{Ra} = 10^5$occurs in case 3 and $d = 1.25$.
- The minimum value of entropy generation is obtained at case 4 while the heater dimensionless spacing is set to $d = 0.95$.
- The effect of nanofluid on both the average Nusselt number and total entropy generation is more pronounced at case 2 ($d = 0.8$) and case 3 when the heater is located at $d = 1.25$.

Consequently, the performances of the six cases can be evaluated in terms of Nu_m/S^*_{gen}, which is defined by Zahmatkesh [22]. So the highest performance concerns case 5 and $d = 0.4$ which the ratio of average Nusselt number to global entropy generation rate is equal to 31,975, and the lowest performance related to case 3 and $\mathrm{d} = 1.25$ that Nu_m/S^*_{gen} is equal to 5,835.

REFERENCES

1. O. Polat and E. Bilgen, Laminar Natural Convection in Inclined Open Shallow Cavities, *Int. J. Ther. Sci.*, Vol. 41, pp. 360–368, 2002.
2. E. Bilgen and H. Oztop, Natural Convection Heat Transfer in Partially Open Inclined Square Cavities, *Int. J. Heat Mass Transfer*, vol. 48, pp. 1470–1479, 2005.
3. A. Koca, Numerical Analysis of Conjugate Heat Transfer in a Partially Open Square Cavity with a Vertical Heat Source, *Int. Commun. Heat Mass Transfer*, vol. 35, pp. 1385–1395, 2008.
4. Y. Stiriba, Analysis of the Flow and Heat Transfer Characteristics for Assisting Incompressible Laminar Flow Past an Open Cavity, *Int. Comms. Heat Mass Transfer*, vol. 35, pp. 901–907, 2008.
5. H. Nouanegue, A. Muftuoglu, and E. Bilgen, Conjugate Heat Transfer by Natural Convection, Conduction and Radiation in Open Cavities, *Int. J. Heat Mass Transfer*, vol. 51, pp. 6054–6062, 2008.
6. N. Kasayapanand, Numerical Modeling of Natural Convection in Partially Open Square Cavities under Electric Field, *Int. Commun. Heat Mass Transfer*, vol. 34, pp. 630–643, 2007.
7. A. H. Mahmoudi, M. Shahi, A. M. Shahedin, and N. Hemati, Numerical Modeling of Natural Convection in an Open Cavity with two Vertical thin Heat Sources Subjected to a Nanofluid, *Int. Commun. Heat Mass Transfer*, vol. 38, pp. 110–118, 2011.
8. Y. M. Xuan and Q. Li, Heat Transfer Enhancement of Nanofluid, *Int. J. Heat Fluid Flow*, vol. 21, pp. 58–64, 2000.

9. K. Khanafer, K. Vafai, and M. Lightstone, Buoyancy-Driven Heat Transfer Enhancement in a Two-Dimensional Enclosure Utilizing Nanofluids, *Int. J. Heat Mass Transfer*, vol. 46, pp. 3639–3653, 2003.
10. G. A. Sheikhzadeh, A. Arefmanesh, M. H. Kheirkhah, and R. Abdollahi, Natural Convection of Cu-Water Nanofluid in a Cavity with Partially Active Side Walls, *Eur. J. Mech. B/Fluids*, vol. 30, pp. 166–176, 2011.
11. S. M. Aminossadati and B. Ghasemi, Natural Convection Cooling of a Localised Heat Source at the Bottom of a Nanofluid-Filled Enclosure, *Eur. J. Mech. B/Fluids*, vol. 28, pp. 630–640, 2009.
12. A. H. Mahmoudi, M. Shahi, A. H. Raouf, and A. Ghasemian, Numerical Study of Natural Convection Cooling of Horizontal Heat Source Mounted in a Square Cavity Filled with Nanofluid, *Int. Comm. Heat Mass Transfer*, vol. 37, pp. 1135–1141, 2010.
13. B. Ghasemi, S. M. Aminossadati, Natural Convection Heat Transfer in an Inclined Enclosure Filled with a Water-Cuo Nanofluid, *Numerical Heat Transfer, Part A: Applications*, vol. 55, pp. 807–823, 2009.
14. B. Ghasemi and S. M. Aminossadati, Periodic Natural Convection in a Nanofluid-Filled Enclosure with Oscillating Heat Flux, *Int. J. Ther. Sci.*, vol. 48, pp. 2063–2073, 2009.
15. Z. Alloui, P. Vasseur, and M. Reggio, Natural Convection of Nanofluids in a Shallow Cavity Heated from Below, *Int. J. Ther. Sci.*, vol. 50, pp. 385–393, 2011.
16. A. H. Mahmoudi, M. Shahi, and A. H. Raouf, Modeling of Conjugated Heat Transfer in a Thickwalled Enclosure Filled with Nanofluid, *Int. Commun. Heat Mass Transfer*, vol. 38, pp. 119–127, 2011.
17. F. Talebi, A. H. Mahmoudi, and M. Shahi, Numerical Study of Mixed Convection Flows in a Square Lid-Driven Cavity Utilizing Nanofluid, *Int. Commun. Heat Mass Transfer*, vol. 37, pp. 79–90, 2010.
18. Z. S. Heris, M. N. Esfahany, and G. Etemad, Numerical Investigation of Nanofluid Laminar Convection Heat Transfer through a Circular Tube, *Numerical Heat Transfer;Part A:Applications*, vol. 52, pp. 1043–1058, 2007.
19. A. Bejan, *Entropy Generation Through Heat and Fluid Flow*, Wiley, New York, 1982.
20. B. S. Yilbas, Laser Short-Pluse Heating of Qold-Silver Assembly: Entropy Generation due to Heat and Electricity Flows in Electron Subsystem, *Numerical Heat Transfer; Part A: Applications*, vol. 49, pp. 873–891, 2006.
21. Y. Varol, H. F. Oztop, and I. Pop, Entropy Generation due to Natural Convection in Non-Uniformly Heated Porous Isosceles Triangular Enclosures at Different Positions, *Int. J. Heat Mass Transfer*, vol. 52, pp. 1193–1205, 2009.
22. I. Zahmatkesh, On the Importance of Thermal Boundary Conditions in Heat Transfer and Entropy Generation for Natural Convection Inside a Porous Enclosure, *Int. J. Ther. Sci.*, vol. 47, pp. 339–346, 2008.
23. R. S. Kaluri, and T. Basak, Entropy Generation Minimization versus Thermal Mixing Due to Natural Convection in Differentially and Discretely Heated Square Cavities, *Numerical Heat Transfer; Part A: Applications*, vol. 58, pp. 475–504, 2010.
24. M. Alipanah, P. Hasannasab, S. F. Hosseinizadeh, and M. Darbandi, Entropy Generation for Compressible Natural Convection with High Gradient Temperature in a Square Cavity, *Int. Commun. Heat Mass Transfer*, vol. 37, pp 1388–1395, 2010.
25. T. H. Ko, Numerical Investigation of Laminar Forced Convection and Entropy Generation in a Helical Coil with Constant Wall Heat Flux, *Numerical Heat Transfer; Part A: Applications*, vol. 49, pp. 257–278, 2006.
26. Y. Feng and C. Kleinstreuer, Nanofluid Convective Heat Transfer in a Parallel-Disk System, *Int. J. Heat Mass Transfer*, vol. 53, pp. 4619–4628, 2010.
27. J. Li and C. Kleinstreuer, Entropy Generation Analysis for Nanofluid Flow in Microchannels, *J. Heat Transfer*, vol. 132, pp. 122401.1–122401.8, 2010.

28. P. K. Singh, K. B. Anoop, T. Sundararajan, and S. K. Das, Entropy Generation Due to Flow and Heat Transfer in Nanofluids, *Int. J. Heat Mass Transfer*, vol. 53, pp. 4757–4767, 2010.
29. H. E. Patel, T. Pradeep, T. Sundararajan, A. Dasgupta, N. Dasgupta, and S. K. Das, A Microconvection Model for Thermal Conductivity of Nanofluid, *Pramana. J. Phys.*, vol. 65, pp. 863–869, 2005.
30. H. C. Brinkman, The Viscosity of Concentrated Suspensions and Solutions, *J. Chem. Phys.*, vol. 20, pp. 571–581, 1952.
31. J. H. Ferziger and M. Peric, *Computational Method for Fluid Dynamics*, Springer-Verlag, New York, 1999.
32. S. V. Patnkar, *Numerical Heat Transfer and Fluid Flow*, Hemisphere, New York, 1980.
33. M. Shahi, Numerical Simulation of 3-Dimensional Steady Flow and Heat Transfer in a Single-Ended Tube, MSc thesis, The University of Semnan, Semnan, Iran, 2009. (In Farsi).
34. G. De Vahl Davis, Natural Convection of Air in a Square Cavity a Bench Mark Numerical Solution, *Int. J. Numeri. Meth. Fluids*, vol. 3, pp. 249–264, 1983.
35. A. K. Santra, S. Sen, and N. Chakraborty, Study of Heat Transfer due to Laminar Flow of Copper–Water Nanofluid through Two Thermally Heated Parallel Plates, *Inter. J. Ther. Sci.*, vol. 48, pp. 391–400, 2009.